Molecular Science

AIMS Molecular Science, 13(2): 205–225.
DOI: 10.3934/molsci.2026011
Received: 04 December 2025
Revised: 05 April 2026
Accepted: 07 April 2026
Published: 21 April 2026

http://www.aimspress.com/journal/Molecular

Research article

miR-32-5p–mediated downregulation of choline kinase alpha promotes apoptosis and reduces migration in MCF7 breast cancer cells

Shaleniprieya Muniandy[1], Sweta Raikundalia[1], Ling Ling Few[1,*], Shuhaila Mat-Sharani[1], Get Bee Yvonne-Tee[1], Nor Fadhilah Kamaruzzaman[2], Chan Yean Yean[3] and Wei Cun See Too[1,*]

[1] School of Health Sciences, Health Campus, Universiti Sains Malaysia, 16150 Kubang Kerian, Kelantan, Malaysia
[2] Nanotechnology in Veterinary Medicine Research Group, Faculty of Veterinary Medicine, Universiti Malaysia Kelantan, 16100 Pengkalan Chepa, Kelantan, Malaysia
[3] Department of Medical Microbiology & Parasitology, School of Medical Sciences, Health Campus, Universiti Sains Malaysia, 16150 Kubang Kerian, Kelantan, Malaysia

* **Correspondence:** Email: fewling@usm.my; stweicun@usm.my; Tel: +6012-5765215; +6017-4337612; Fax: +609-7677515; +609-7677515.

Abstract: Choline kinase alpha (CHKA) plays an important role in phospholipid metabolism and is frequently overexpressed in several cancers, where it contributes to tumor growth and survival. In this study, we investigated whether microRNA-32-5p (miR-32-5p) regulates CHKA expression and influences malignant phenotypes in human breast cancer cells. Bioinformatic prediction and luciferase reporter assays suggested a potential interaction between miR-32-5p and the *CHKA* 3' UTR. Transfection of miR-32-5p into MCF7 cells significantly reduced *CHKA* mRNA and CHKA protein expression. This downregulation was associated with increased apoptosis, G0/G1 cell-cycle arrest, and reduced migration of MCF7 cells. Reduced phosphorylation of ERK and mTOR was also observed, suggesting decreased activation of MAPK/mTOR signaling pathways. In contrast, although *CHKA* expression was reduced in non-tumorigenic MCF10A cells, apoptosis was not induced. These findings indicate that miR-32-5p regulates *CHKA* expression and suppresses malignant phenotypes in breast cancer cells, highlighting its potential role in modulating *CHKA*-associated signaling pathways.

Keywords: miR-32-5p; microRNAs; gene regulation; choline kinase alpha; breast cancer

1. Introduction

Choline kinase (CHK) functions as an essential component of the metabolic pathways responsible for phospholipid production in cells by converting choline into phosphocholine in an ATP-dependent reaction. This step marks the beginning of the CDP-choline pathway, which ultimately produces phosphatidylcholine (PC), the major phospholipid component of eukaryotic membranes. Human choline kinase diversity stems from *CHKA* and *CHKB* genes, which together encode three separate enzyme isoforms [1]. CHKB, produced from the *CHKB* gene, is vital for proper mitochondrial integrity, muscle formation, and bone regulation [2]. Meanwhile, CHKA1 and CHKA2 are the products of *CHKA* through alternative splicing [1]. Choline kinase alpha (CHKA) plays a central role in cancer-associated metabolic reprogramming by regulating phosphocholine production and membrane biosynthesis, processes essential for rapid tumor cell proliferation. In addition to its metabolic function, CHKA has also been implicated in the regulation of key oncogenic signaling pathways, highlighting its dual role in tumor progression [3]. Increased CHKA activity has been consistently associated with tumor development, enhanced proliferation, and malignant progression across multiple cancer types [4–7]. Elevated CHKA expression and activity facilitate increased PC synthesis to sustain rapid cancer cell growth [8].

CHKA has been reported to contribute to the activation of MAPK and PI3K/AKT signaling pathways that support cancer cell viability and proliferation. Early evidence demonstrated that CHKA regulates these pathways in cancer cells such as MDA-MB-468 breast adenocarcinoma [9], followed by studies showing that inhibition of CHKA attenuates MAPK and PI3K/AKT signaling in HeLa cells [7]. Further investigations confirmed the role of CHKA in oncogenic signaling in hepatocellular carcinoma [10], and subsequent work demonstrated that CHKA inhibition induces apoptosis through activation of AMPK and repression of mTORC1 signaling in leukemia T cells [11]. More recent studies have extended these findings to malignant B and T cells [12]. Collectively, these findings highlight the role of CHKA in linking metabolic activity to key survival signaling pathways in cancer cells, as summarized in recent reviews [4].

The activity of CHKA supports multiple fundamental cellular events, including growth, differentiation, programmed cell death, and regulation of the cell cycle [13]. Its expression levels and enzymatic activity, together with its product phosphocholine, are pivotal biomarkers for cancer diagnosis and the evaluation of therapeutic efficacy [14]. Owing to its elevated expression across multiple cancers, CHKA has emerged as a promising therapeutic target, spurring the development of numerous CHKA inhibitors [15]. Yet, the factors governing *CHKA* transcription and post-transcriptional regulation, including potential microRNA (miRNA) involvement, are far from fully elucidated. Several miRNAs have been reported to regulate CHKA expression, including miR-876-5p and miR-367-3p [16,17]. More recently, miR-32-5p has also been implicated in CHKA regulation in cervical cancer cells [18].

Previous studies have demonstrated that inhibition or downregulation of CHKA selectively impairs tumor cell survival while exerting minimal effects on non-tumorigenic cells, with tumor cells undergoing apoptosis, whereas normal cells exhibit limited or reversible effects, highlighting CHKA as a promising metabolic target in cancer therapy [19,20]. However, the post-transcriptional regulation of CHKA by specific miRNAs and the downstream signaling consequences of this regulation remain incompletely understood. In this study, we investigate the regulatory interaction between miR-32-5p and CHKA in breast cancer cells and evaluate its functional impact on apoptosis, cell cycle progression,

migration, and MAPK/mTOR signaling pathways.

miRNAs, typically about 21 nucleotides long, function as non-coding regulators that silence genes by triggering mRNA decay or preventing protein synthesis [21]. They play crucial roles in cell differentiation, immune regulation, apoptosis, and tumorigenesis [22]. Aberrant miRNA expression is common in cancer, making miRNA profiling an important diagnostic and prognostic tool [23]. Several miRNAs are being tested clinically as biomarkers for disease classification, monitoring, and therapeutic modulation [24]. Research into miRNA mimics and anti-miRNA constructs is also advancing, particularly in breast cancer therapy [24]. In breast cancer, microRNA-mediated regulation of apoptosis-related targets such as BCL-2 further highlights the importance of miRNA networks in tumor progression and therapeutic response [25].

This study examined human miR-32-5p, a microRNA with important regulatory roles. Originating from the precursor MI0000090 on chromosome 9q31.3 (NCBI NR_029506), the mature form (5'-UAUUGCACAUUACUAAGUUGCA-3') is listed in miRBase as MIMAT0000090. miR-32-5p has been implicated in cancer by modulating diverse gene targets. For instance, it suppresses TLDC1 to inhibit proliferation and migration in pancreatic adenocarcinoma [26] but promotes gastric cancer cell growth via downregulation of DSC2 [27]. miR-32-mediated suppression of FBXW7 has also been reported to enhance breast cancer cell proliferation and migration [28].

In this study, we investigated how *CHKA* expression is influenced by miR-32-5p in MCF7 cancer cells. Introducing miR-32-5p into these cells led to a marked decrease in mRNA of *CHKA* levels, increased apoptotic activity, and inhibited cell migration. Collectively, these results demonstrate that miR-32-5p exerts a suppressive influence on key malignant traits in breast cancer and may represent a promising therapeutic candidate for targeting CHKA-associated oncogenic pathways.

2. Materials and methods

2.1. Prediction and validation of miRNA–CHKA 3' UTR interactions

Potential miRNAs predicted to bind to the 3' UTR of *CHKA* mRNA were screened with miRDB (https://www.mirdb.org), microRNA.org (http://www.microrna.org), TargetScan (https://www.targetscan.org), and DIANA microT-CDS (https://dianalab.e-ce.uth.gr/microt_webserver/) with default parameters (miRDB ≥ 80; microRNA.org alignment > 140 and $\Delta G < -20$ kcal/mol; TargetScan context ++ score < -0.2; DIANA ≥ 0.7). Candidates predicted by all tools were further analyzed for minimum free energy (MFE) of binding using RNAfold, Kinefold, and mFold. miRNA–*CHKA* binding sites were manually inspected to optimize seed complementarity and minimize bulges. The selected miRNAs were then evaluated for seed region types [29], target site classification [30], and site context characteristics [31] to ensure specificity and effectiveness.

2.2. Cell line maintenance, miRNA transfection, and reporter assays reagents

MCF7 cells (ATCC® HTB-22™) were cultured in DMEM supplemented with 10% fetal bovine serum and penicillin–streptomycin. MCF10A cells (ATCC® CRL-10317™) were maintained in DMEM/F12 containing 5% horse serum, 20 ng/mL EGF, 0.5 μg/mL hydrocortisone, 10 μg/mL insulin, and 1% antibiotic (penicillin–streptomycin). All cell lines were grown at 37 °C in a humidified incubator with 5% CO_2. MCF7 cells are a human breast adenocarcinoma cell line commonly used as

a model of tumorigenic breast epithelial cells, whereas MCF10A cells are non-tumorigenic human mammary epithelial cells that serve as a representative model of normal breast tissue. The use of these two cell lines enables comparison between cancerous and non-tumorigenic cellular responses to miRNA-mediated regulation.

Transfection reagents included the synthetic hsa-miR-32-5p mimic (5'-UAUUGCACAUUACUAAGUUGCA-3'), a sequence-specific inhibitor, and two control mimics: Housekeeping Positive Control #2 and Negative Control #1 (5'-UCACAACCUCCUAGAAAGAGUAGA-3'). These oligonucleotides were purchased from Dharmacon or Applied Biological Materials and reconstituted in 1× siRNA buffer. Reporter activity was assessed using a firefly luciferase plasmid (OriGene, catalog number: SC212759) in which the *CHKA* 3' UTR was cloned.

2.3. Transfection of oligonucleotides

Using Lipofectamine 3000 (Invitrogen, Thermo Fisher Scientific), MCF7 cultures were transfected with a panel of oligonucleotides, which included miR-32-5p mimic, its inhibitor, and the control miRNAs, alongside the pMirTarget plasmid encoding the *CHKA* 3' UTR fused to firefly luciferase. Transfections for luciferase assays were conducted in 96-well plates, and those for qRT-PCR and western blot in 24-well plates, with cells seeded at 1×10^4 and 1×10^5 cells/well, respectively, to reach 70%–80% confluence [17].

Plasmids (200 ng) and miRNA mimics/inhibitors (25 nM) were first prepared in Opti-MEM™ (Thermo Fisher Scientific). These nucleic acids were then combined with an equal volume of Lipofectamine 3000 and incubated for 20 min to enable complex formation prior to being applied to the cells. The incubation was carried out at room temperature.

2.4. Firefly luciferase assay

MCF7 cells were seeded into 96-well plates and subsequently co-introduced with the pMirTarget construct carrying the *CHKA* 3' UTR, the miR-32-5p mimic or its inhibitor (Applied Biological Materials, Richmond, Canada), together with Negative Control #1 (Dharmacon, CO, USA). After transfection, the luminescence of the Dual-Glo luciferase system (Promega, WI, USA) was quantified using a GloMax 20/20 luminometer (Promega). Each experiment was analyzed in triplicate. Firefly luciferase readings were normalized to the negative control to calculate relative changes in reporter activity.

2.5. Extraction of RNA and quantitative assessment of CHKA expression

RNA was recovered from miR-32-5p-transfected MCF7 cells using the Total RNA Isolation kit (Thermo Fisher Scientific, MA, USA) and then treated with the RNase-Free DNase set (Qiagen, Hilden, Germany). RNA quantity and purity were determined using a NanoDrop ND-1000 spectrophotometer (Thermo Fisher Scientific). For cDNA synthesis, 1 μg of RNA was converted to first-strand cDNA with the RevertAid™ H Minus kit (Thermo Fisher Scientific) following incubation at 42 °C for 1 h.

Quantitative PCR analysis was carried out using Power SYBR™ Green Master Mix (Thermo Fisher Scientific) on an ABI Prism 7500 platform. The reactions were run under the following thermal

profile: an initial denaturation at 95 ℃ for 10 min, followed by 40 cycles of 95 ℃ for 10 s and 60 ℃ for 1 min. Gene-specific primers included *CHKA* (forward: 5'-TCAGAGCAAACATCCGGAAGT-3'; reverse: 5'-GGCGTAGTCCATGTACCCAAAT-3'), as well as *GAPDH*, *YWHAZ*, and *RPS18*. Changes in *CHKA* transcript abundance were calculated using the $2^{-\Delta\Delta Ct}$ approach [32], where expression values were adjusted relative to the geometric mean of *YWHAZ* and *RPS18*, employed as internal reference genes.

2.6. Quantification of apoptosis via Muse™ Annexin V & dead cell assay

To evaluate apoptosis, transfected cells were processed with the Muse™ Annexin V & Dead Cell Assay (Merck Millipore) and analyzed using the Muse™ cell analyzer. Cells were harvested by trypsinization, washed once with PBS, and resuspended in complete DMEM at a density of 1×10^6 cells/mL. The assay was performed by mixing the suspension with Annexin V reagent (1:1 ratio). The mixture was incubated at room temperature, in light-shielded conditions, for 30 min before it was analyzed on the Muse™ analyzer.

2.7. Cell cycle assay

Cell cycle profiling of MCF7 cells transfected with the miRNA mimic was performed using the Muse® Cell Cycle kit (Merck Millipore) in combination with the Muse™ cell analyzer. Following transfection, cells were collected by trypsinization, rinsed with PBS, and preserved in 70% ethanol at −20 ℃ for fixation. For staining, approximately 5×10^5 cells were incubated with the Muse™ cell cycle reagent for 30 min at room temperature, protected from light, and subsequently analyzed on the Muse™ system.

2.8. Scratch wound healing assay

A P20 pipette tip was used to make a uniform scratch on near-confluent transfected MCF7 cells in 6-well plates. After two PBS rinses, cells were maintained in serum-free medium. A DINO EYE eyepiece camera (AnMo Electronics, Taiwan) was used to take pictures of wound closures at designated time intervals. Gap distances were quantified using ImageJ version 1.49b (https://imagej.net/ij/). Brightness and contrast were adjusted uniformly across all images.

2.9. Western blot analyses

Seventy-two hours post-transfection, MCF7 cells were treated with ProteoJET™ lysis reagent (Thermo Fisher Scientific, USA) to obtain protein extracts, which were quantified by the Bradford method. Equivalent protein quantities were resolved on 12% SDS-PAGE gels and subsequently transferred onto nitrocellulose membranes. The blots were blocked in 5% skim milk prepared in TBST and probed overnight with primary antibodies specific to CHKA (ABclonal), phospho-ERK, total ERK, phospho-mTOR, total mTOR (Cell Signaling Technology, USA), and β-actin, the loading control. Because ERK1/2 and β-actin have similar molecular weights, membranes were sequentially stripped and reprobed using validated stripping conditions, and complete removal of the previous antibody signal was verified prior to reprobing to ensure accurate detection and quantification. After incubation

with HRP-linked goat anti-rabbit IgG (Sigma-Aldrich), signals were developed using the SuperSignal™ West Femto detection reagent and imaged with a FUSION FX system (Vilber Lourmat, France). Densitometric analysis of the protein bands was carried out in ImageJ version 1.49b, and all experiments were independently reproduced three times.

2.10. Statistical evaluation of experimental results

Student's t-test or one-way ANOVA (Tukey's HSD), for multiple-group evaluations, were used to test for statistical comparisons. Differences were considered significant at $p < 0.05$. All analyses were conducted with SPSS v22.0 and GraphPad Prism 10. Data are presented as mean ± SEM from three independent biological replicates.

3. Results

3.1. miR-32-5p fulfills silico criteria for targeting the 3' UTR of CHKA *mRNA*

In silico screening resulted in the prediction of 40 miRNA candidates that targeted the *CHKA* 3' UTR by at least two of four prediction tools (miRDB, microRNA.org, TargetScan, and DIANA microT-CDS), while six miRNAs were consistently identified by all tools (Figure 1). Four of these shared identical seed sequences, forming one miRNA family.

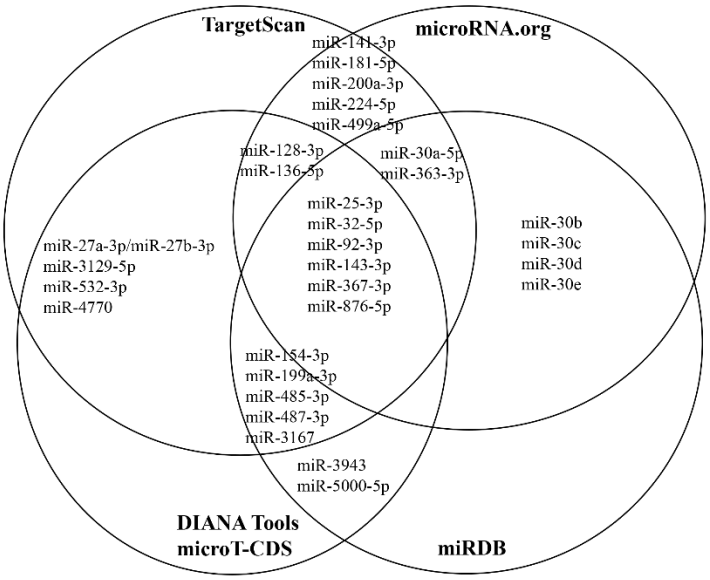

Figure 1. Comparative Venn diagram showing miRNAs jointly predicted by miRDB, microRNA.org, TargetScan, and DIANA microT-CDS.

Among the candidates, miR-32-5p met all selection criteria, including optimal minimum free energy (MFE), seed complementarity, and site efficacy. It binds nucleotides 1753–1771 of the *CHKA* 3' UTR with a canonical 8-mer seed match and 5' dominance (Figure 2). The predicted interaction exhibited MFE values of –1.70, –2.40, and –2.50 kcal/mol using RNAfold, Kinefold, and mFold, respectively, supported by two Watson–Crick base pairs within the 12–17 nt target region (Figure 2).

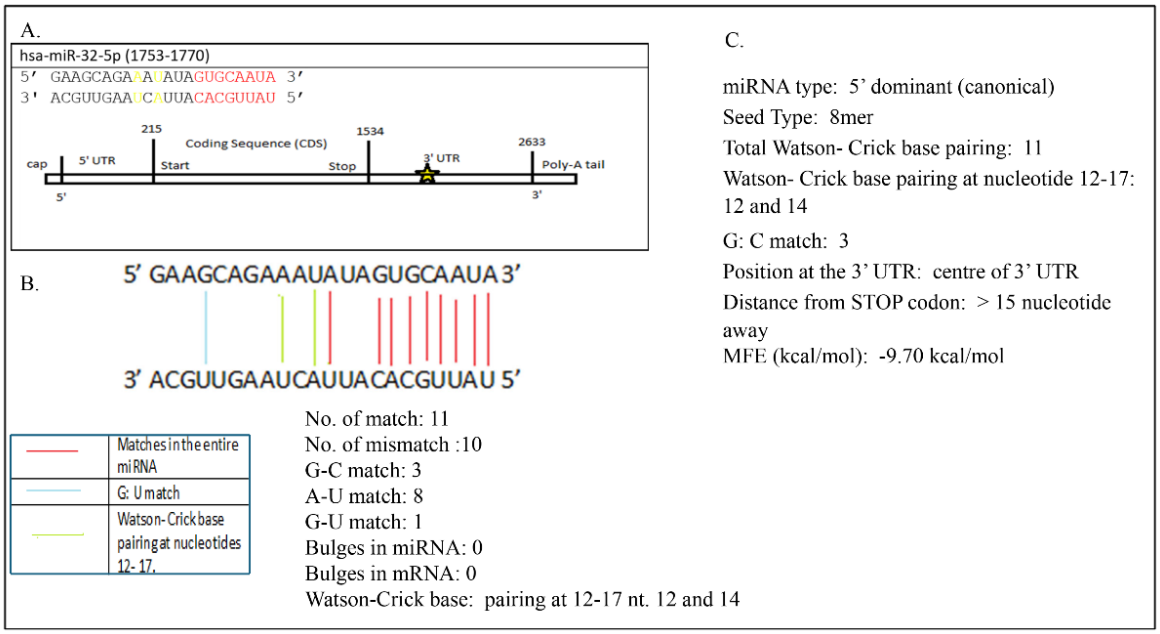

Figure 2. miR-32-5p complementary site within the *CHKA* 3' untranslated region. (A) miR-32-5p binding site on *CHKA* 3' UTR. (B) Watson–Crick nucleotide base pairing between hsa-miR-32-5p microRNA and its binding site on *CHKA* mRNA. (C) Eight attributes of miRNA/mRNA outcome: 1) miRNA site type, 2) seed type, 3) Watson–Crick base pairing, 4) nucleotides 12–17 engage in typical Watson–Crick base pairing, 5) G:C match, 6) position at the 3' UTR, 7) distance from stop codon, and 8) the minimum free energy (MFE).

3.2. Reporter assay demonstrating miR-32-5p-mediated regulation of CHKA

As shown in Figure 3, transfection of the miR-32-5p mimic resulted in a clear reduction in luciferase activity compared with the negative control, suggesting that miR-32-5p interacts with the *CHKA* 3' UTR and modulates its expression. Conversely, introduction of the miR-32-5p inhibitor produced an increase in luciferase activity, consistent with relief of miRNA-mediated repression. Co-transfection of the mimic and inhibitor resulted in an intermediate response. The partial restoration of *CHKA* expression following co-transfection with the miR-32-5p inhibitor suggests that the inhibitory effect may be incomplete and that additional regulatory factors may influence *CHKA* expression in MCF7 cells. Although the observed changes did not reach statistical significance, the overall trend is consistent with miR-32-5p-dependent regulation of *CHKA*.

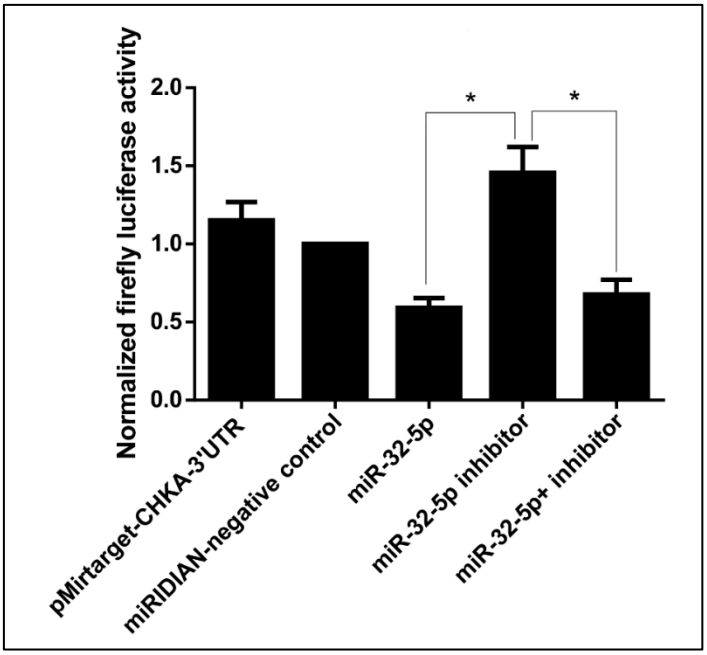

Figure 3. Verification of miR-32-5p targeting the *CHKA* 3' UTR. MCF7 cells were co-transfected with the pMirTarget-*CHKA*-3' UTR reporter and the indicated miRNA mimics or inhibitors. Luciferase output was measured following each treatment condition. Asterisks denote significant differences (one-way ANOVA with Tukey's HSD, $p < 0.05$).

3.3. miR-32-5p suppresses CHKA *gene expression in MCF7 cells*

Figure 4 shows that *CHKA* mRNA expression was significantly higher in MCF7 cells compared with the non-tumorigenic MCF10A cells. Relative expression analysis using the $2^{-\Delta\Delta Ct}$ method revealed several-fold higher *CHKA* transcript levels in MCF7 cells, consistent with the elevated CHKA expression commonly observed in breast cancer cells. To further assess the effect of miR-32-5p on *CHKA* expression following baseline comparison (Figure 4), transfection experiments were performed. Upon transfection with miR-32-5p mimic, MCF7 cells exhibited a significantly reduced *CHKA* mRNA level (by 53%) compared to the negative control (Figure 5). When the mimic and inhibitor were delivered together, *CHKA* expression dropped by 62%, whereas treatment with the inhibitor alone resulted in a 29% reduction. Notably, the incomplete recovery of *CHKA* expression following co-transfection with the miR-32-5p inhibitor suggests that the inhibitory efficiency may be limited under the experimental conditions, particularly in the presence of exogenous miRNA mimic, and that additional regulatory mechanisms may contribute to the modulation of *CHKA* expression in MCF7 cells.

While the inhibitor showed a pattern resembling the luciferase findings (Figure 3), hinting at complex regulatory interactions, these findings establish miR-32-5p as a potent repressor of *CHKA* expression in MCF7 cells. Future validation, including separate inhibitor controls and measurement of miR-32-5p levels post-transfection, is warranted to clarify these interactions.

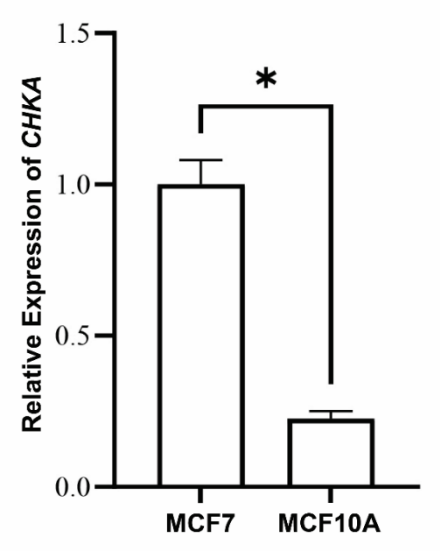

Figure 4. Relative *CHKA* expression in MCF7 and MCF10A cells. Analysis by qRT-PCR demonstrated that MCF7 cells expressed significantly higher levels of *CHKA* mRNA compared with MCF10A cells ($p < 0.05$).

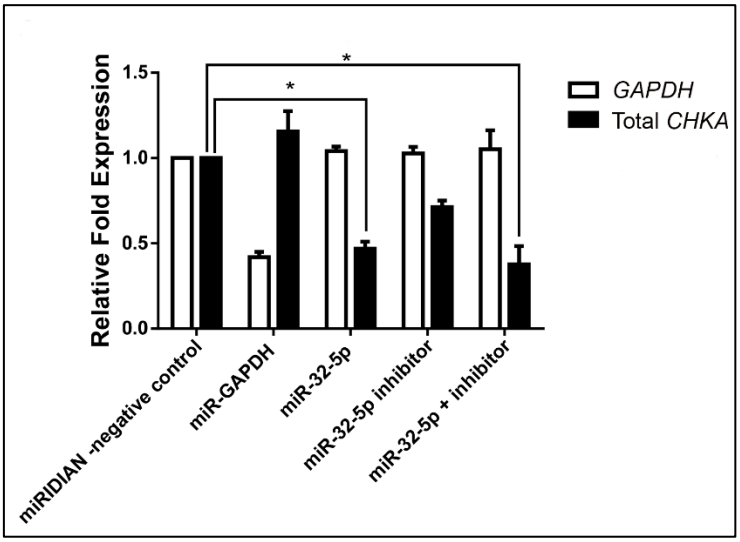

Figure 5. Impact of miR-32-5p mimic transfection on *CHKA* gene expression in MCF cells. The cells were exposed to 25 nM miR-32-5p mimic; subsequent changes in *CHKA* expression levels were then quantified by qRT-PCR after 48 h. The standard error of the mean (SEM) from three replicates is shown as error bars. Asterisks denote significant differences relative to the miRIDIAN negative control (one-way ANOVA with Tukey's HSD, $p < 0.05$).

3.4. Downregulation of CHKA *by miR-32-5p promotes apoptosis and induces cell cycle arrest in MCF7 cells*

Transfection of miR-32-5p into MCF7 cells markedly increased apoptosis to 58.9%, compared to

16.0% in untransfected cells (Figure 6A), indicating that *CHKA* downregulation by miR-32-5p promotes cell death.

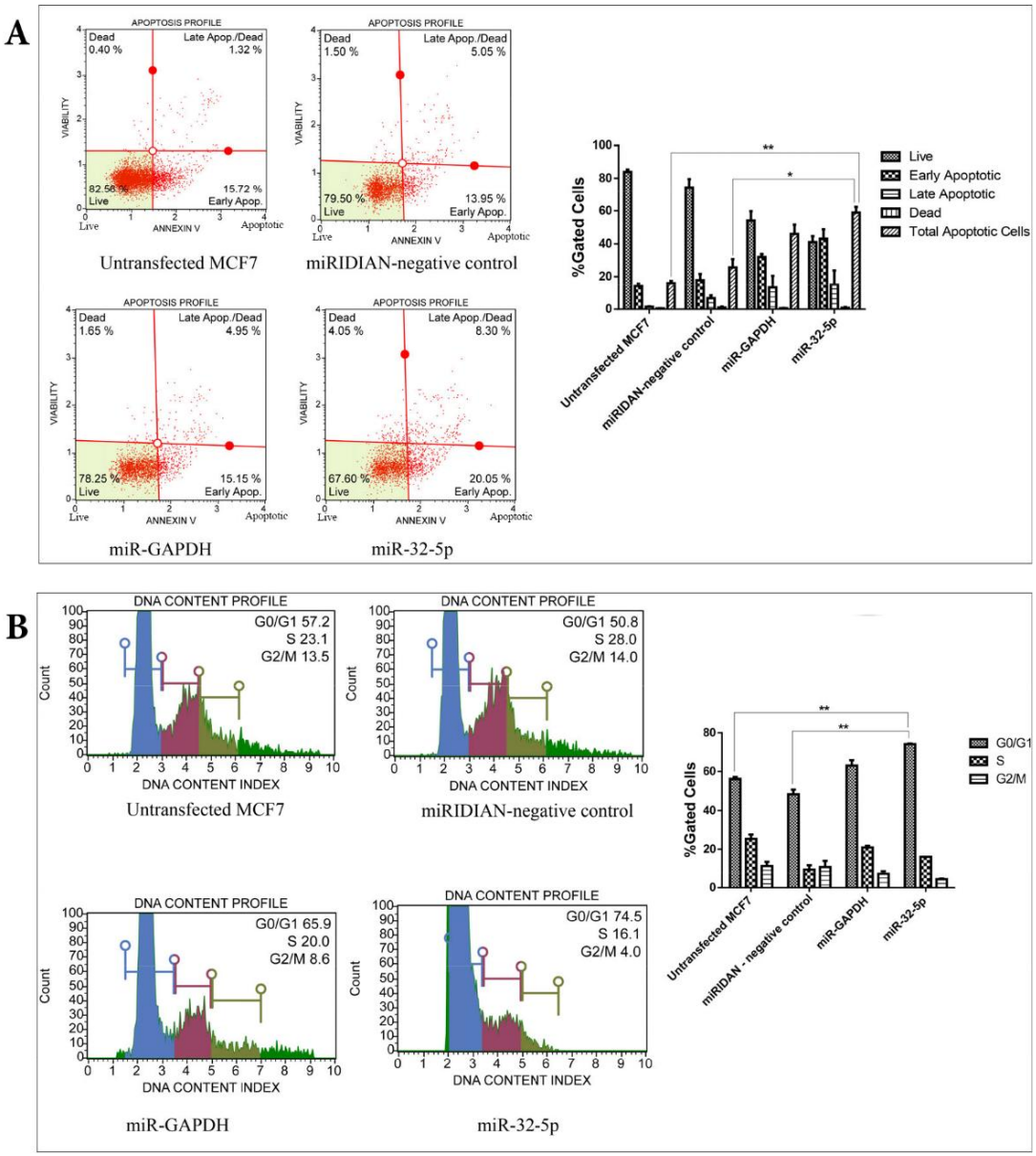

Figure 6. Changes in apoptosis and cell cycle dynamics induced by miR-32-5p in MCF7 cells. (A) Introduction of the miR-32-5p mimic (25 nM, 48 h) markedly increased the proportion of apoptotic cells. Statistical comparisons were carried out using one-way ANOVA with Tukey's post hoc test (*$p < 0.05$; **$p < 0.01$). (B) miR-32-5p transfection causes a pronounced accumulation of cells in the G0/G1 phase, accompanied by reduced proportions in the S and G2/M compartments. One-way ANOVA with Tukey's post hoc test was used for statistical evaluation (*$p < 0.05$; **$p < 0.01$).

Upon miR-32-5p transfection, the majority of MCF7 cells were found in G0/G1 (72.16%), while markedly smaller fractions populated the S (17.53%) and G2/M (7.26%) phases, highlighting a strong

G0/G1 arrest compared to the control population (Figure 6B). An increase in the G0/G1 population suggests that miR-32-5p disrupts normal cell cycle transit, contributing to the suppressed growth of MCF7 breast cancer cells. These observations support a dual role for miR-32-5p in triggering apoptosis while limiting cell cycle advancement in MCF7 cells, highlighting its potential functional significance and the importance of clarifying its underlying regulatory mechanisms.

The relatively elevated apoptotic levels observed in cells transfected with the miR-GAPDH positive control likely reflect efficient suppression of the *GAPDH* gene, a key enzyme involved in glycolysis and cellular energy metabolism. Disruption of *GAPDH* expression can induce metabolic stress and apoptosis; therefore, this control was included primarily to confirm transfection efficiency rather than to serve as a biological comparator for miR-32-5p.

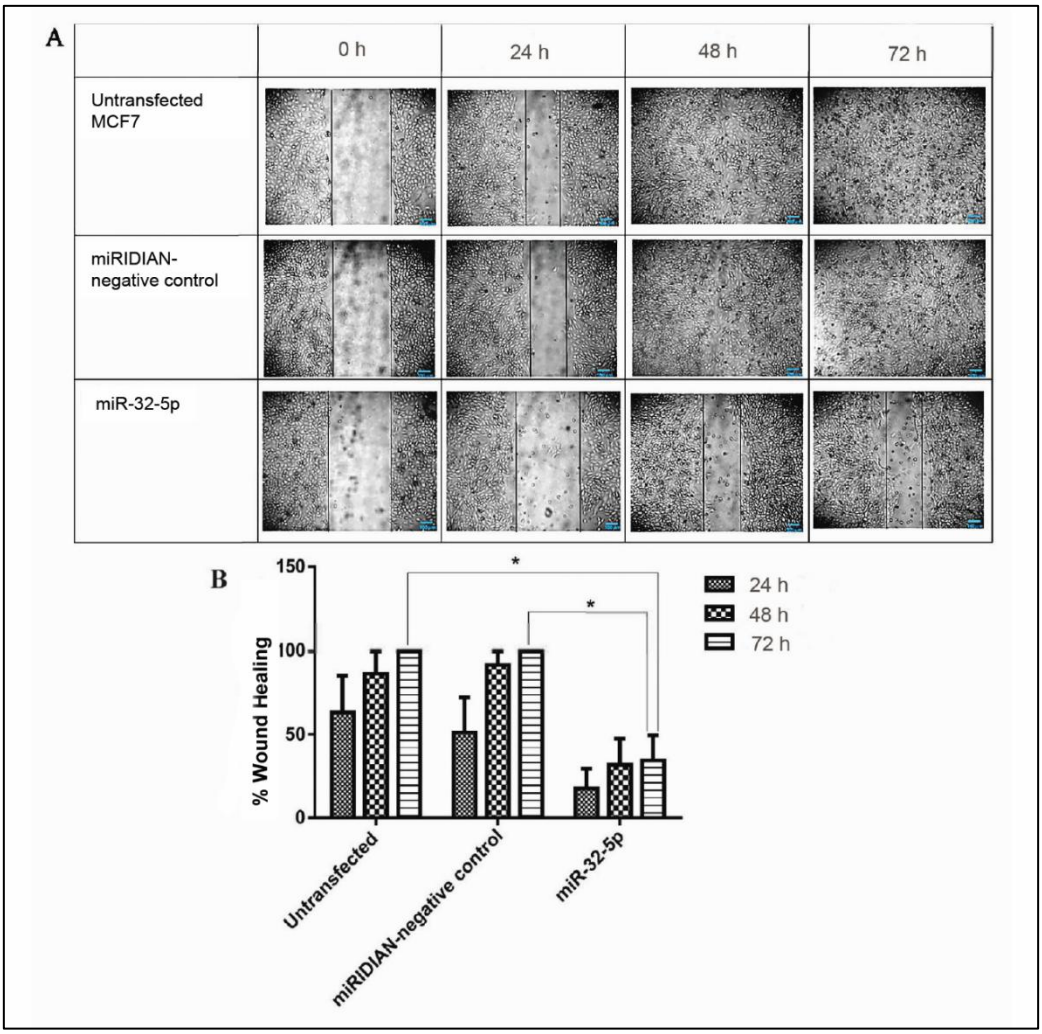

Figure 7. miR-32-5p suppresses migration of MCF7 cells in a wound healing assay. (A) Representative images of wound closure in untreated control, negative control, and miR-32-5p-transfected MCF7 cells captured at the indicated time points. Wound boundaries are outlined to facilitate comparison of migration between treatment groups. Scale bar = 100 μm. (B) Quantitative analysis of wound closure over time, calculated using ImageJ software. Data represent mean ± SEM from three independent experiments. Significant differences between miR-32-5p-treated cells and controls are indicated (*$p < 0.05$).

3.5. Suppression of CHKA *by miR-32-5p limits MCF7 cell migration*

Wound healing assays revealed that miR-32-5p-transfected MCF7 cells exhibited markedly reduced migration, with only 30.34% wound closure after 72 h, compared to complete closure in both control and untransfected cells (Figure 7). The observations suggest that miR-32-5p-mediated suppression of *CHKA* significantly impairs the migratory ability of MCF7 breast cancer cells.

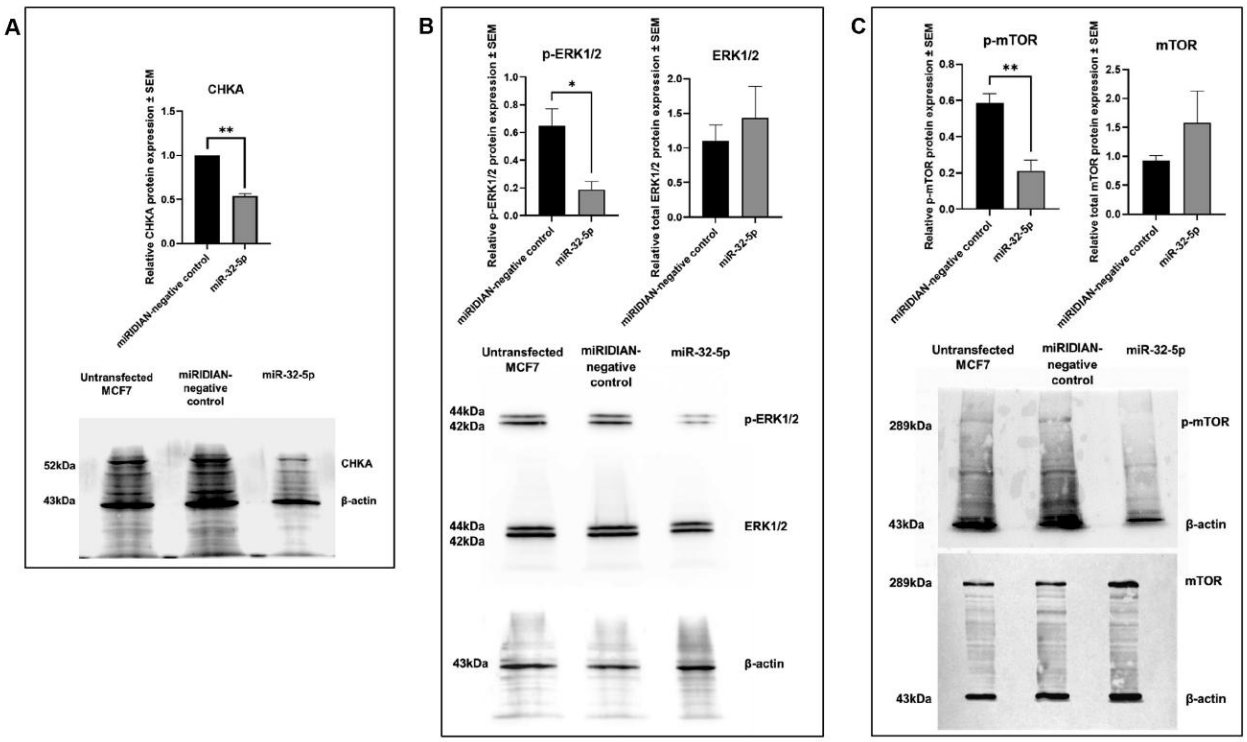

Figure 8. miR-32-5p reduces the levels of CHKA, p-ERK1/2, and p-mTOR protein expression in MCF7 cells. (A) MCF7 cells treated with the miR-32-5p mimic showed a pronounced reduction in CHKA protein levels relative to the miRIDIAN negative control group. (B) Exposure to miR-32-5p lowered the abundance of phosphorylated ERK1/2, whereas total ERK1/2 levels were not affected. (C) p-mTOR level was also significantly decreased by miR-32-5p, with no significant effect on total mTOR level. Bar charts represent the mean ± SEM of protein expression, normalized to either β-actin (for CHKA, total ERK1/2, and mTOR) or corresponding total protein (for p-ERK1/2 and p-mTOR) from three biological replicates. The statistical significance was evaluated using Student's t-test (*$p < 0.05$, **$p < 0.01$). Images displayed are representative of Western blots generated across three independent experiments. Molecular weights: β-actin, 43 kDa; CHKA, 52 kDa; ERK1/2 and p-ERK1/2, 44/42 kDa; p-mTOR, 289 kDa. Due to the similar molecular weights of total ERK1/2, p-ERK1/2, and β-actin, a stripping and reprobing approach was used to detect these targets sequentially on the membrane. Due to the similar molecular weights of ERK1/2, p-ERK1/2, and β-actin, membranes were sequentially stripped and reprobed. Complete removal of the previous antibody signal was verified before each reprobing step to ensure reliable detection. Differences in blot background and image dimensions were due to repeated probing and technical variations in image acquisition.

3.6. miR-32-5p inhibits CHKA and downstream survival signaling pathways

A noticeable decline in the expression of CHKA protein was observed in miR-32-5p-transfected MCF7 cells (Figure 8), as shown by the western blot, supporting CHKA as a direct target of miR-32-5p. Since MAPK and mTOR pathways are well-known regulators for migration and apoptosis [33,34], their involvement was assessed. Consistent with CHKA suppression, phosphorylated ERK (p-ERK) and phosphorylated mTOR (p-mTOR) levels were significantly decreased in miR-32-5p-treated cells (Figure 8), indicating attenuation of cell survival signaling.

3.7. miR-32-5p downregulates CHKA *without inducing apoptosis in MCF10A cells*

Exposure of non-tumorigenic MCF10A cells to 25 μM miR-32-5p for 48 h produced a substantial decline in *CHKA* mRNA abundance, approximately 63% lower than that observed in negative control–treated cells (Figure 9). This level of downregulation was comparable to the 53% decrease observed in MCF7 cells ($p = 0.4063$) (Figure 5). Successful transfection was verified by a 98% suppression of *GAPDH* using the miR-GAPDH positive control. However, apoptosis analysis using the Muse™ cell analyzer revealed no increase in apoptotic cells following miR-32-5p transfection (Figure 10), indicating that miR-32-5p-dependent suppression of *CHKA* triggers apoptosis in MCF7 cancer cells while sparing non-tumorigenic MCF10A cells.

The lower apoptotic response observed in miR-GAPDH-transfected MCF10A cells compared with MCF7 cells may reflect differences in metabolic dependence between tumorigenic and non-tumorigenic cells. Cancer cells often exhibit enhanced reliance on glycolysis for energy production, making them more susceptible to apoptosis following suppression of key glycolytic enzymes such as GAPDH.

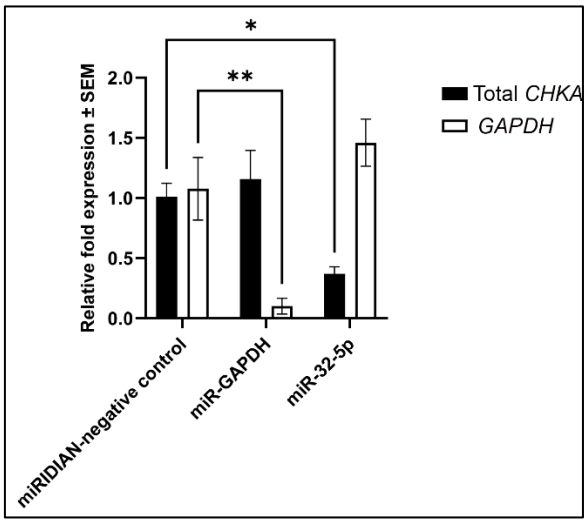

Figure 9. miR-32-5p downregulates *CHKA* expression in MCF-10A cells. Relative fold expression ± SEM of *CHKA* and *GAPDH* levels after transfection of the negative control, *GAPDH*-targeting positive control, and miR-32-5p into MCF10A cells, measured after 48 h by qRT-PCR. *CHKA* and *GAPDH* expressions were normalized to *YWHAZ* and *RPS18* housekeeping genes. miR-32-5p suppressed *CHKA* levels in MCF10A with 63% reduction. Data were analyzed using one-way ANOVA followed by post hoc Tukey HSD test (*$p < 0.05$, **$p < 0.01$).

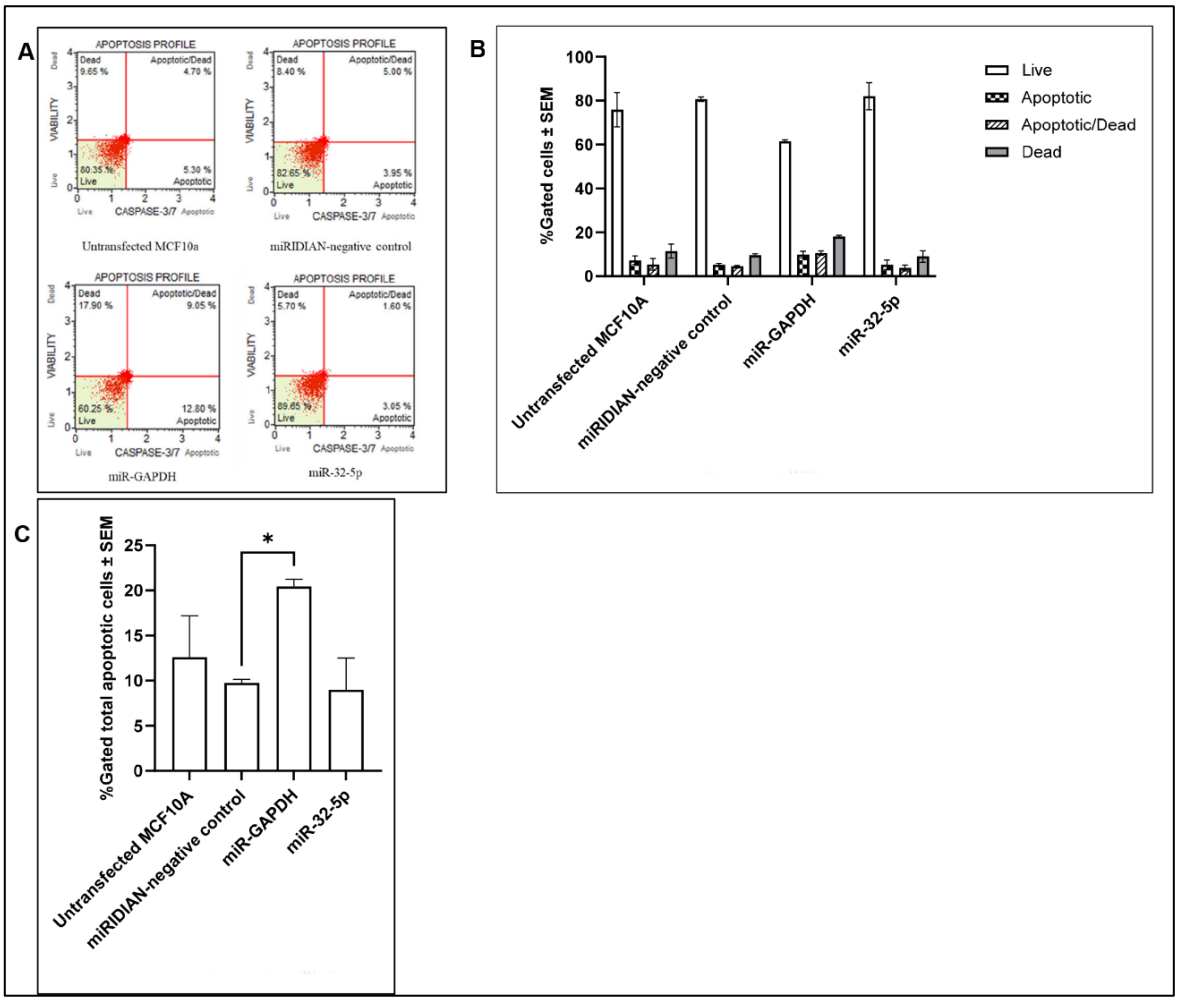

Figure 10. Transfection with miR-32-5p did not trigger apoptosis in MCF10A cells. (A) Quadrants of cell populations distinguish into live, apoptotic, late apoptotic/dead, and dead cells after miR-32-5p transfection in MCF10A cells. (B) Quantification of cell populations presented as mean ± SEM from three independent assays. (C) Total apoptotic cells after transfection. The proportion of total apoptotic cells did not differ significantly between miR-32-5p-treated and negative-control groups ($p > 0.05$; one-way ANOVA with Tukey's HSD).

4. Discussion

CHKA is increasingly recognized as a key metabolic regulator and therapeutic target in cancer [3], supporting processes involved in cellular transformation and the initiation of tumor growth. Its overexpression is a significant factor in multiple cancers, prompting investigations into strategies to inhibit its activity or reduce its expression as potential anticancer therapies [15,35]. Early studies reported elevated CHKA enzymatic activity in 39% of breast carcinoma samples [36], and subsequent research expanded this observation to other cancers, detecting CHKA overexpression in 56% of lung, 48% of prostate, and 47% of colon cancers [6]. Increased CHKA activity has also been documented in pancreatic [37], ovarian [38], and endometrial cancers [39].

A retrospective study of patients with non-small-cell lung cancer who underwent surgical

resection revealed a significant prognostic impact of CHKA expression. When tumor CHKA expression increased to approximately double that of adjacent normal tissue, patient prognosis worsened substantially, with four-year survival dropping to 49% compared with 71% in those with reduced CHKA expression [40]. In breast cancer, elevated CHKA enzymatic activity has been associated with more aggressive tumor phenotypes and shows a negative correlation with estrogen receptor expression, implying that CHKA may contribute to reduced responsiveness to endocrine therapies such as tamoxifen [36]. Collectively, these data emphasize CHKA's central involvement in malignancy and its potential value for prognosis and targeted intervention.

The differential response of tumorigenic and non-tumorigenic cells to CHKA inhibition has been previously reported, with CHKA inhibition causing reversible cell-cycle arrest in normal/non-tumorigenic cells but apoptosis or loss of viability in tumor cells, supporting the concept that cancer cells exhibit greater dependence on choline metabolism for proliferation and survival [19,20]. Our findings are consistent with these observations and further demonstrate that miR-32-5p-mediated downregulation of CHKA produces selective apoptotic effects in breast cancer cells while sparing non-tumorigenic epithelial cells, suggesting that microRNA-mediated regulation of CHKA may contribute to this metabolic vulnerability.

CHKA has emerged as a promising target for precision medicine strategies, as its inhibition can selectively impair tumor cell viability while sparing normal cells. Various approaches, including small-molecule inhibitors and RNA interference-based strategies, have been developed to target CHKA in cancer [3]. Biodegradable dextran nanopolymers have been employed to deliver siRNA against *CHKA* in breast cancer, demonstrating the potential of RNAi- and miRNA-based therapeutic strategies [41].

In this context, our study explored how miRNAs regulate *CHKA* expression. Despite their size, these RNAs function as potent modulators of gene expression, primarily operating through post-transcriptional mechanisms. By targeting *CHKA*, miRNAs could significantly alter cellular metabolism, proliferation, and survival [42–45]. Our findings contribute to understanding the interplay between miRNAs and *CHKA*, providing insight into how these molecules modulate gene expression within the broader regulatory networks that govern tumor development. These findings should be interpreted in the context of the complex regulatory network governing CHKA expression, as multiple factors in addition to miR-32-5p may contribute to its modulation in cancer cells.

Analysis using prediction tools indicated a robust miR-32-5p recognition site within the *CHKA* 3' UTR. This prediction was supported by mirSVR scores and minimum free energy (MFE) values, which are key indicators of miRNA silencing efficiency [46,47]. These computational methods are valuable for prioritizing experimentally testable hypotheses, reducing the time and resources required for empirical validation.

The data clearly demonstrates that introducing miR-32-5p into MCF7 cells leads to substantial decreases in *CHKA* mRNA and CHKA protein expression. These molecular effects coincide with elevated apoptotic activity and diminished cell motility, supporting the role of miR-32-5p as a regulatory miRNA with tumor-suppressive functions in CHKA-driven pathways.

Numerous studies have established the capacity of miRNAs to suppress cell proliferation and induce apoptosis across diverse cancer models. For instance, miR-28-5p contributes to curcumin's antiproliferative and pro-apoptotic actions in diffuse large B-cell lymphoma [48], while miR-21 targets TIMP3 to elicit similar effects in LPS-treated fibroblasts [49]. Evidence from triple-negative breast cancer models suggests that miR-32-5p prevents progression via ring finger protein 38 (RNF38) suppression, whereas lncRNA HNF1A-AS1 promotes tumor cell growth by sponging miR-32-5p and

preventing its regulatory activity [50]. Together, these observations highlight the broader tumor-suppressive capabilities of miR-32-5p and align with our findings that its repression of *CHKA* attenuates breast cancer cell growth, migration, and survival.

miR-32-5p exhibits diverse roles across malignancies, with its function varying according to cellular context. In certain tumors, it behaves as an oncogenic miRNA. For example, it contributes to key oncogenic processes in oral squamous cell carcinoma, including increased proliferation, invasive behavior, and induction of epithelial–mesenchymal transition [51], and its elevated expression in ovarian cancer promotes enhanced growth and motility [52]. In contrast, miR-32-5p can also function as a tumor suppressor, limiting migration and invasion via SMAD3 repression in non-small-cell lung cancer [53], as well as downregulating HOXB8 to inhibit cervical cancer progression [54]. Additional layers of regulatory diversity have been reported in MCF7 cells, in which miR-362-5p restricts cell growth and reduces invasive behavior through suppression of CYLD [55]. Interestingly, previous investigations have reported that miR-32 drives tumor cell growth and migration and simultaneously suppresses apoptotic activity through downregulation of the tumor-suppressor FBXW7 [28], a pattern opposite to our observations that miR-32-5p restricts MCF7 cell growth and motility via CHKA. These divergent findings underscore the highly tissue- and gene-specific nature of miR-32-5p regulation across cancers. In line with previous findings that miR-367-3p reduces the expression of CHKA, inhibiting migration and triggering apoptosis [17], our results further indicate that miR-32-5p may also influence downstream signaling pathways involved in cell survival. The dual role of miR-32-5p reported across different tumor types highlights the context-dependent nature of microRNA regulation and suggests that its therapeutic application may be limited without careful consideration of tumor-specific molecular networks. Therefore, although our results demonstrate that miR-32-5p suppresses CHKA expression and promotes apoptosis in MCF7 breast cancer cells, further studies across multiple cancer models will be required before its therapeutic potential can be fully established.

Previous studies have shown that RNAi-mediated downregulation of CHKA attenuates MAPK signaling [7] and reduces proliferation in HeLa cells [13]. However, unlike RNAi, miR-32-5p is not exclusively specific to CHKA, and its transfection may influence multiple targets involved in MAPK signaling and cell proliferation. Our target prediction using TargetScan, miRDB, and miRmap identified 139 common predicted genes. Gene ontology and KEGG pathway enrichment analyses via Enrichr showed that these targets are involved in regulating the p38MAPK cascade, MAPK kinase binding, and MAPK/mTOR signaling pathways. Future studies should examine whether the MAPK/mTOR pathway underlies the pro-apoptotic and anti-migratory actions of miR-32-5p and contributes to its effects on cell-cycle regulation.

Analysis of data from the sRNA Expression Atlas (SEA) showed that miR-32-5p is more abundant in MCF7 breast cancer cells (223.31 RPM) than in non-tumorigenic MCF10A cells (125.79 RPM). When considered alongside the elevated CHKA expression detected in MCF7, this differential miRNA pattern highlights the need to further dissect how miR-32-5p and CHKA interact in malignant versus normal breast cell contexts.

5. Conclusions

Consistent with previous reports describing the selective sensitivity of cancer cells to CHKA inhibition, our findings further demonstrate that miR-32-5p represents an additional regulatory mechanism capable of modulating CHKA expression and downstream oncogenic signaling pathways.

These findings identify miR-32-5p as a regulator of CHKA expression and associated signaling pathways in breast cancer cells. While the results provide insight into microRNA-mediated control of CHKA-dependent oncogenic processes, additional studies in diverse cancer models and in vivo systems will be necessary to determine whether miR-32-5p could be safely exploited for therapeutic purposes.

Author contributions

WCST and LLF contributed to the study conception and design. Material preparation, data collection and analysis were performed by SM and SR. The first draft of the manuscript was written by LLF, SM and SR. LLF, WCST, SMS, CYY, GBYT, and NFK provided critical revisions to the manuscript, supervised the research process, and secured funding. All authors read and approved of the final manuscript.

Use of Generative-AI tools declaration

The authors declare they have not used Artificial Intelligence (AI) tools in the creation of this article.

Acknowledgments

This research was funded by the Universiti Sains Malaysia Bridging Grant with Project No: R501-LR-RND003-0000002377-0000. We gratefully acknowledge the technical support provided by the laboratory personnel of the School of Health Sciences, USM, as well as the staff of the Central Research Laboratory, School of Medical Sciences, USM.

Conflict of interest

The authors declare that they have no competing interests.

References

1. Arlauckas SP, Popov AV, Delikatny EJ (2016) Choline kinase alpha—Putting the ChoK-hold on tumor metabolism. *Prog Lipid Res* 63: 28–40. https://doi.org/10.1016/j.plipres.2016.03.005
2. Chang CC, Few LL, Konrad M, et al. (2016) Phosphorylation of human choline kinase Beta by protein kinase A: Its impact on activity and inhibition. *PLoS One* 11: e0154702. https://doi.org/10.1371/journal.pone.0154702
3. Lacal JC, Zimmerman T, Campos JM. (2021) Choline kinase: An unexpected journey for a precision medicine strategy in human diseases. *Pharmaceutics* 13: 788. https://doi.org/10.3390/pharmaceutics13060788
4. Korbecki J, Bosiacki M, Kupnicka P, et al. (2025) Choline kinases: Enzyme activity, involvement in cancer and other diseases, inhibitors. *Int J Cancer* 156: 1314–1325. https://doi.org/10.1002/ijc.35286

5. Glunde K, Bhujwalla ZM, Ronen SM (2011) Choline metabolism in malignant transformation. *Nat Rev Cancer* 11: 835–848. https://doi.org/10.1038/nrc3162
6. de Molina AR, Rodríguez-González A, Gutiérrez R, et al. (2002) Overexpression of choline kinase is a frequent feature in human tumor-derived cell lines and in lung, prostate, and colorectal human cancers. *Biochem Biophys Res Commun* 296: 580–583. https://doi.org/10.1016/s0006-291x(02)00920-8
7. Yalcin A, Clem B, Makoni S, et al. (2010) Selective inhibition of choline kinase simultaneously attenuates MAPK and PI3K/AKT signaling. *Oncogene* 29: 139–149. https://doi.org/10.1038/onc.2009.317
8. Clem BF, Clem AL, Yalcin A, et al. (2011) A novel small molecule antagonist of choline kinase-α that simultaneously suppresses MAPK and PI3K/AKT signaling. *Oncogene* 30: 3370–3380. https://doi.org/10.1038/onc.2011.51
9. Chua BT, Gallego-Ortega D, de Molina AR, et al. (2009) Regulation of Akt(ser473) phosphorylation by Choline kinase in breast carcinoma cells. *Mol Cancer* 8: 131. https://doi.org/10.1186/1476-4598-8-131
10. Lin XM, Hu L, Gu J, et al. (2017) Choline kinase α mediates interactions between the epidermal growth factor receptor and mechanistic target of rapamycin complex 2 in hepatocellular carcinoma cells to promote drug resistance and xenograft tumor progression. *Gastroenterology* 152: 1187–1202. https://doi.org/10.1053/j.gastro.2016.12.033
11. Mariotto E, Bortolozzi R, Volpin I, et al. (2018) EB-3D a novel choline kinase inhibitor induces deregulation of the AMPK-mTOR pathway and apoptosis in leukemia T-cells. *Biochem Pharmacol* 155: 213–223. https://doi.org/10.1016/j.bcp.2018.07.004
12. Gokhale S, Xie P (2021) ChoK-full of potential: Choline kinase in B cell and T cell malignancies. *Pharmaceutics* 13: 911. https://doi.org/10.3390/pharmaceutics13060911
13. Gruber J, See Too WC, Wong MT, et al. (2012) Balance of human choline kinase isoforms is critical for cell cycle regulation. *FEBS J* 279: 1915–1928. https://doi.org/10.1111/j.1742-4658.2012.08573.x
14. Wu G, Vance DE (2010) Choline kinase and its function. *Biochem Cell Biol* 88: 559–564. https://doi.org/10.1139/O09-160
15. Schiaffino-Ortega S, Baglioni E, Mariotto E, et al. (2016) Design, synthesis, crystallization and biological evaluation of new symmetrical biscationic compounds as selective inhibitors of human Choline Kinase α1 (ChoKα1). *Sci Rep* 6: 23793. https://doi.org/10.1038/srep23793
16. Ayub Khan SM, Few LL, See Too WC (2018) Downregulation of human choline kinase α gene expression by miR-876-5p. *Mol Med Rep* 17: 7442–7450. https://doi.org/10.3892/mmr.2018.8762
17. Raikundalia S, Sa'Dom SAFM, Few LL, et al. (2021) MicroRNA-367-3p induces apoptosis and suppresses migration of MCF-7 cells by downregulating the expression of human choline kinase α. *Oncol Lett* 21: 183. https://doi.org/10.3892/ol.2021.12444
18. Raikundalia S, Few LL, Hassan SA, et al. (2024) Choline kinase and miR-32-5p: A crucial interaction promoting apoptosis and delaying wound repair in cervical cancer cells. *AIMS Biophys* 11: 281–295. https://doi.org/10.3934/biophy.2024016
19. Rodríguez-González A, de Molina AR, Bañez-Coronel M et al. (2005) Inhibition of choline kinase renders a highly selective cytotoxic effect in tumour cells through a mitochondrial independent mechanism. *Int J Oncol* 26: 999-1008.

20. Bañez-Coronel M, de Molina AR, Rodríguez-González A et al. (2008) Choline kinase alpha depletion selectively kills tumoral cells. *Curr Cancer Drug Targets* 8: 709-719. https://doi.org/10.2174/156800908786733432
21. Gebert LFR, MacRae IJ (2019) Regulation of microRNA function in animals. *Nat Rev Mol Cell Biol* 20: 21–37. https://doi.org/10.1038/s41580-018-0045-7
22. Hirschberger S, Hinske LC, Kreth S (2018) MiRNAs: Dynamic regulators of immune cell functions in inflammation and cancer. *Cancer Lett* 431: 11–21. https://doi.org/10.1016/j.canlet.2018.05.020
23. Lan H, Lu H, Wang X, et al. (2015) MicroRNAs as potential biomarkers in cancer: opportunities and challenges. *Biomed Res Int* 2015: 125094. https://doi.org/10.1155/2015/125094
24. Shah V, Shah J (2020) Recent trends in targeting miRNAs for cancer therapy. *J Pharm Pharmacol* 72: 1732–1749. https://doi.org/10.1111/jphp.13351
25. Mayuri K, Vickram S, Anand T, et al. (2025) MicroRNA-mediated regulation of BCL-2 in breast cancer. *AIMS Mol Sci* 12: 32–48. https://doi.org/10.3934/molsci.2025003
26. Yuan P, Tang C, Chen B, et al. (2021) miR-32-5p suppresses the proliferation and migration of pancreatic adenocarcinoma cells by targeting TLDC1. *Mol Med Rep* 24: 752. https://doi.org/10.3892/mmr.2021.12392
27. Sun C, Huang LG, Leng B, et al. (2025) MicroRNA-32-5p promotes the proliferation and metastasis of gastric cancer cells. *Sci Rep* 15: 2282. https://doi.org/10.1038/s41598-025-86367-3
28. Xia W, Zhou J, Luo H, et al. (2017) MicroRNA-32 promotes cell proliferation, migration and suppresses apoptosis in breast cancer cells by targeting FBXW7. *Cancer Cell Int* 17: 14. https://doi.org/10.1186/s12935-017-0383-0
29. McGeary SE, Lin KS, Shi CY, et al. (2019) The biochemical basis of microRNA targeting efficacy. *Science* 366: eaav1741. https://doi.org/10.1126/science.aav1741
30. Brennecke J, Stark A, Russell RB, et al. (2005) Principles of microRNA-target recognition. *PLoS Biol* 3: e85. https://doi.org/10.1371/journal.pbio.0030085
31. Grimson A, Farh KK-H, Johnston WK, et al. (2007) MicroRNA targeting specificity in mammals: determinants beyond seed pairing. *Mol Cell* 27: 91–105. https://doi.org/10.1016/j.molcel.2007.06.017
32. Livak KJ, Schmittgen TD (2001) Analysis of relative gene expression data using real-time quantitative PCR and the $2^{-\Delta\Delta Ct}$ method. *Methods* 25: 402–408. https://doi.org/10.1006/meth.2001.1262
33. Shen Z, Xue D, Wang K, et al. (2022) Metformin exerts an antitumor effect by inhibiting bladder cancer cell migration and growth, and promoting apoptosis through the PI3K/AKT/mTOR pathway. *BMC Urol* 22: 79. https://doi.org/10.1186/s12894-022-01027-2
34. Yue J, López JM (2020) Understanding MAPK signaling pathways in apoptosis. *Int J Mol Sci* 21. https://doi.org/10.3390/ijms21072346
35. Wang N, Brickute D, Braga M, et al. (2021) Novel non-congeneric derivatives of the choline kinase Alpha inhibitor ICL-CCIC-0019. *Pharmaceutics* 13: 1078. https://doi.org/10.3390/pharmaceutics13071078
36. de Molina AR, Gutiérrez R, Ramos MA, et al. (2002) Increased choline kinase activity in human breast carcinomas: Clinical evidence for a potential novel antitumor strategy. *Oncogene* 21: 4317–4322. https://doi.org/10.1038/sj.onc.1205556

37. Penet MF, Shah T, Bharti S, et al. (2015) Metabolic imaging of pancreatic ductal adenocarcinoma detects altered choline metabolism. *Clin Cancer Res* 21: 386–395. https://doi.org/10.1158/1078-0432.CCR-14-0964
38. Iorio E, Ricci A, Bagnoli M, et al. (2010) Activation of phosphatidylcholine cycle enzymes in human epithelial ovarian cancer cells. *Cancer Res* 70: 2126–2135. https://doi.org/10.1158/0008-5472.CAN-09-3833
39. Trousil S, Lee P, Pinato DJ, et al. (2014) Alterations of choline phospholipid metabolism in endometrial cancer are caused by choline kinase alpha overexpression and a hyperactivated deacylation pathway. *Cancer Res* 74: 6867–6877. https://doi.org/10.1158/0008-5472.CAN-13-2409
40. de Molina AR, Sarmentero-Estrada J, Belda-Iniesta C, et al. (2007) Expression of choline kinase alpha to predict outcome in patients with early-stage non-small-cell lung cancer: A retrospective study. *Lancet Oncol* 8: 889–897. https://doi.org/10.1016/S1470-2045(07)70279-6
41. Chen Z, Krishnamachary B, Bhujwalla ZM (2016) Degradable dextran nanopolymer as a carrier for choline kinase (ChoK) siRNA cancer therapy. *Nanomaterials* 6: 34. https://doi.org/10.3390/nano6020034
42. Chen H, Xie G, Luo Q, et al. (2023) Regulatory miRNAs, circRNAs and lncRNAs in cell cycle progression of breast cancer. *Funct Integr Genomics* 23: 233. https://doi.org/10.1007/s10142-023-01130-z
43. Darvish L, Bahreyni Toossi MT, Azimian H, et al. (2023) The role of microRNA-induced apoptosis in diverse radioresistant cancers. *Cell Signal* 104: 110580. https://doi.org/10.1016/j.cellsig.2022.110580
44. Ma L (2016) MicroRNA and metastasis. In: *Advances in cancer research*, 132: 165–207. https://doi.org/10.1016/bs.acr.2016.07.004
45. Petri BJ, Klinge CM (2020) Regulation of breast cancer metastasis signaling by miRNAs. *Cancer Metastasis Rev* 39: 837–886. https://doi.org/10.1007/s10555-020-09905-7
46. Oliveira AC, Bovolenta LA, Nachtigall PG, et al. (2017) Combining results from distinct MicroRNA target prediction tools enhances the performance of analyses. *Front Genet* 8: 59. https://doi.org/10.3389/fgene.2017.00059
47. Zheng Z, Reichel M, Deveson I, et al. (2017) Target RNA secondary structure is a major determinant of miR159 efficacy. *Plant Physiol* 174: 1764–1778. https://doi.org/10.1104/pp.16.01898
48. Kang T, Sun WL, Lu XF, et al. (2020) MiR-28-5p mediates the anti-proliferative and pro-apoptotic effects of curcumin on human diffuse large B-cell lymphoma cells. *J Int Med Res* 48: 1-13. https://doi.org/10.1177/0300060520943792
49. Li JX, Li Y, Xia T, et al. (2021) miR-21 Exerts Anti-proliferative and Pro-apoptotic Effects in LPS-induced WI-38 Cells via Directly Targeting TIMP3. *Cell Biochem Biophys* 79: 781–790. https://doi.org/10.1007/s12013-021-00987-w
50. Yang J, Niu H, Chen X (2021) GATA1-activated HNF1A-AS1 facilitates the progression of triple-negative breast cancer via sponging miR-32-5p to upregulate RNF38. *Cancer Manag Res* 2021: 1357–1369. https://doi.org/10.2147/CMAR.S274204
51. Qin SY, Li B, Chen M, et al. (2022) MiR-32-5p promoted epithelial-to-mesenchymal transition of oral squamous cell carcinoma cells via regulating the KLF2/CXCR4 pathway. *Kaohsiung J Med Sci* 38: 120–128. https://doi.org/10.1002/kjm2.12450

52. Zeng S, Liu S, Feng J, et al. (2020) MicroRNA-32 promotes ovarian cancer cell proliferation and motility by targeting SMG1. *Oncol Lett* 20: 733–741. https://doi.org/10.3892/ol.2020.11624
53. Zhang JX, Yang W, Wu JZ, et al. (2021) MicroRNA-32-5p inhibits epithelial-mesenchymal transition and metastasis in lung adenocarcinoma by targeting SMAD family 3. *J Cancer* 12: 2258–2267. https://doi.org/10.7150/jca.48387
54. Liu YJ, Zhou HG, Chen LH, et al. (2019) MiR-32-5p regulates the proliferation and metastasis of cervical cancer cells by targeting HOXB8. *Eur Rev Med Pharmacol Sci* 23: 87–95. https://doi.org/10.26355/eurrev_201901_16752
55. Ni F, Gui Z, Guo Q, et al. (2016) Downregulation of miR-362-5p inhibits proliferation, migration and invasion of human breast cancer MCF7 cells. *Oncol Lett* 11: 1155–1160. https://doi.org/10.3892/ol.2015.3993

AIMS Press